

Modification of coordination networks through a photoinduced charge transfer process†

Cite this: DOI: 10.1039/c3sc52745j

Timothy L. Easun, Junhua Jia, Thomas J. Reade, Xue-Zhong Sun, E. Stephen Davies, Alexander J. Blake, Michael W. George* and Neil R. Champness*

A metal-bearing coordination network synthesised from Re(2,2'-bipyridine-5,5'-dicarboxylate)(CO)₃Cl bridging ligands and Cu(II) nodes, $[\{Cu(DMF)(H_2O)[LRe(CO)_3Cl]\} \cdot DMF]_{\infty}$ **ReCu**, undergoes an irreversible photoinduced charge transfer process. We demonstrate using time-resolved IR spectroscopy the nature of this photoinduced process and how, under suitable conditions, it is possible to initiate irreversible modification of the crystal through induction of the charge transfer process. As a result we are able to use the photoinduced process, which arises purely as a result of the structure of the coordination network, to write on crystals.

Received 1st October 2013
Accepted 28th November 2013

DOI: 10.1039/c3sc52745j

www.rsc.org/chemicalscience

Introduction

The study of coordination networks and the closely related¹ metal-organic frameworks (MOFs)² has seen many advances in recent years^{3–9} in combination with these materials finding a variety of applications, ranging from magnetic materials³ to gas storage⁴ and more recently in photochemical applications, from inducing photochemical reactions within frameworks,^{5–8} initiating energy transfer processes^{9–11} and sensing guest molecules.^{12,13} All of these applications rely on the principle that coordination networks represent structures with their components regularly positioned in three-dimensional space.^{1,2} We have been developing this simple premise to organise photoactive components as inherent building-blocks of coordination networks.⁵

Our previous studies exploited the use of a M(L)(CO)₃X (M = Re, Mn, H₂L = 2,2'-bipyridine-5,5'-dicarboxylate; X = Cl, Br) moiety as a ligand building-block within a coordination network through reaction with Mn(II) salts to afford a three-dimensional network $\{Mn(DMF)_2[C_{12}H_6N_2O_4Re(CO)_3Cl]\}_{\infty}$ **ReMn**.⁵ Through incorporation of the M(diimine)(CO)₃X building-block within the network environment the photo-physics of the moiety are modified, leading to comparisons between such materials and enzyme-like environments.¹⁴ In this study we develop these concepts by constructing a coordination network which positions the photoactive building-block, Re(H₂L)(CO)₃Cl, adjacent to a redox active metal cation that is capable of acting as an electron acceptor, in this case Cu(II). This

approach opens up the possibility of photo-induced charge transfer within the framework. Previous studies of photoactive MOFs have facilitated chemical changes of the network material but this has not been achieved through a charge transfer process, thus this represents the first example of a photoinduced redox-reaction within a crystalline network structure.

The opportunity to photoinduce a charge-transfer process raises the possibility of directly influencing local structure within a crystal through the use of light. The consequences of such a process depend upon whether the photoinduced process is reversible or not, and, indeed, previous studies have demonstrated reversible photoinduced linkage isomerism.¹⁵ If the process is irreversible, and a permanent chemical change is brought about, then it should be possible to use light to modify the crystalline material, effectively allowing a process by which one can “write” on, or in, a crystal. Such approaches have been used to modify the shape and colour of crystalline materials¹⁶ but we demonstrate how this can be achieved through the design and synthesis of a coordination network, indicating a method for the possible design of photo-modifiable materials combining multiple designed properties.

Experimental

Synthesis of $[\{Cu(DMF)(H_2O)[LRe(CO)_3Cl]\} \cdot DMF]_{\infty}$, **ReCu**

ReL(CO)₃Cl (L = 2,2'-bipyridine-5,5'-dicarboxylic acid) (18 mg, 0.037 mmol) was dissolved in EtOH–C₆H₅Me (1 : 1, 1 mL) and added to a solution of CuCl₂ (6.5 mg, 0.049 mmol) in DMF (1 mL). The resulting solution was kept in the dark and some solvent allowed to evaporate over a period of two weeks to form green crystals of the product. Found: C, 32.42; H, 2.86; N, 7.11; calc. for $[\{Cu(DMF)(H_2O)[LRe(CO)_3Cl]\} \cdot DMF]_{\infty}$: C, 32.51; H, 2.84; N, 7.23%.

School of Chemistry, University of Nottingham, University Park, Nottingham, NG7 2RD, UK. E-mail: Neil.Champness@nottingham.ac.uk; Mike.George@nottingham.ac.uk; Fax: +44 (0)1159513563

† Electronic supplementary information (ESI) available: Further experimental data and discussion. CCDC 861593. For ESI and crystallographic data in CIF or other electronic format see DOI: 10.1039/c3sc52745j

The crystal patterning was performed using a confocal Horiba–Jobin–Yvon LabRAM Raman microscope as follows: the initial sample map was recorded over a $50 \times 50 \mu\text{m}$ region with a $3.5 \mu\text{m}$ spacing between points using a $50\times$ objective. Spectra at each point were collected by recording 5 acquisitions of 5 seconds duration each using a 785 nm diode laser operating at low power (*ca.* 0.3 mW) with the spectrometer centred at 1350 cm^{-1} . The Duoscan mirrors of the microscope were then used to sweep the 325 nm laser repeatedly back and forth along a $100 \mu\text{m}$ line (time to cover line 0.27 s) across the short axis of the crystal for a period of 2 h . This irradiation was repeated along a line at 45° to the first. The Raman spectra mapping was then repeated as above (ESI†).

Crystal data for **ReCu**: $\text{C}_{18}\text{H}_{15}\text{ClCuN}_3\text{O}_9\text{Re}\cdot\text{C}_3\text{H}_7\text{NO}$, $M = 775.62$, monoclinic, Cc, $a = 10.0183(7)$, $b = 27.574(2)$, $c = 9.4686(6) \text{ \AA}$, $\beta = 95.291(1)^\circ$, $U = 2604.5(3) \text{ \AA}^3$, $Z = 4$, $T = 150(2) \text{ K}$, 7561 independent reflections ($R_{\text{int}} = 0.033$). Refinement of 356 parameters converged at final $R_1 = 0.0292$, $wR_2 = 0.0620$, GOF = 0.91 .

Results and discussion

Reaction of $\text{Re}(\text{H}_2\text{L})(\text{CO})_3\text{Cl}$ with CuCl_2 in DMF/EtOH/toluene solution followed by slow evaporation over a period of two weeks gave green needle-shaped crystals of $[\{\text{Cu}(\text{DMF})(\text{H}_2\text{O})[\text{LRe}(\text{CO})_3\text{Cl}]\}_\infty] \cdot \text{DMF}_\infty$, **ReCu**. The X-ray structural determination reveals that the $\text{Re}(\text{diimine})(\text{CO})_3\text{Cl}$ moiety retains an octahedral fac arrangement. Each $\text{Cu}(\text{II})$ centre is bound by two carboxylate donors, a DMF and a water molecule in a square-planar geometry, leading to the formation of one-dimensional chains of alternating $\text{Re}(\text{diimine})(\text{CO})_3\text{Cl}$ groups and $\text{Cu}(\text{II})$ centres (Fig. 1). Further long range, Jahn–Teller distorted, Cu–O interactions ($\text{Cu–O} = 2.54 \text{ \AA}$) between the $\text{Cu}(\text{II})$ cation and a carboxylate of a neighbouring chain leads to the formation of a 10^3 srs three-dimensional net¹⁷ in which both $\text{Cu}(\text{II})$ cations and the $\text{Re}(\text{diimine})(\text{CO})_3\text{Cl}$ groups act as three-connected nodes (Fig. 1).

$\text{Re}(\text{diimine})(\text{CO})_3\text{Cl}$ complexes are commonly luminescent in solution, excitation into the $^1\text{MLCT}$ absorption band typically leading to emission from a well characterised $^3\text{MLCT}$ excited state. In our previously reported example, **ReMn**, we found that incorporation of the $\text{Re}(\text{diimine})(\text{CO})_3\text{Cl}$ unit into a rigid network resulted in no detectable emission in the crystalline solid state.⁵ **ReCu** is also non-emissive on the nanosecond timescale, so to further investigate the interplay of excited states within the material we undertook a series of photochemical and TRIR measurements (Scheme 1). The infrared spectrum of crystalline **ReCu** was measured as a powder in a KBr disc and was found to be consistent with the fac-isomer of the $\text{Re}(\text{diimine})(\text{CO})_3\text{Cl}$ unit identified crystallographically, $\nu(\text{CO})$ bands being observed at 2011 , 1909 and 1884 cm^{-1} (with a small shoulder visible at *ca.* 1900 cm^{-1}).

Fig. 2a shows the TRIR difference spectra recorded at 3 ps , 500 ps and 6 ns after laser excitation. The ground-state $\nu(\text{CO})$ bands are bleached and in the 3 ps spectrum new bands are observed shifted to higher energy (2043 , 1972 and 1958 cm^{-1}) relative to the parent bands. This is consistent with the

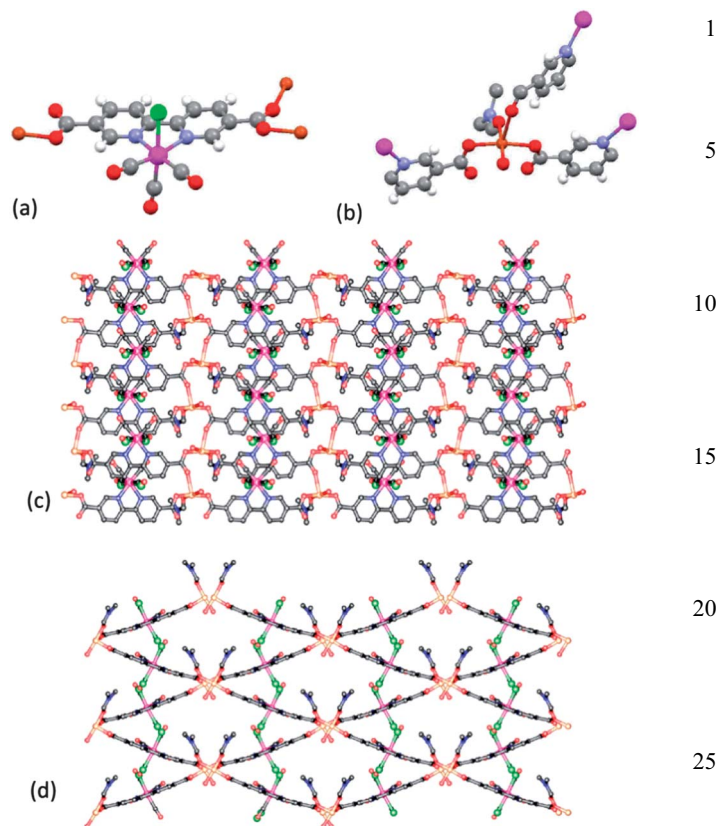
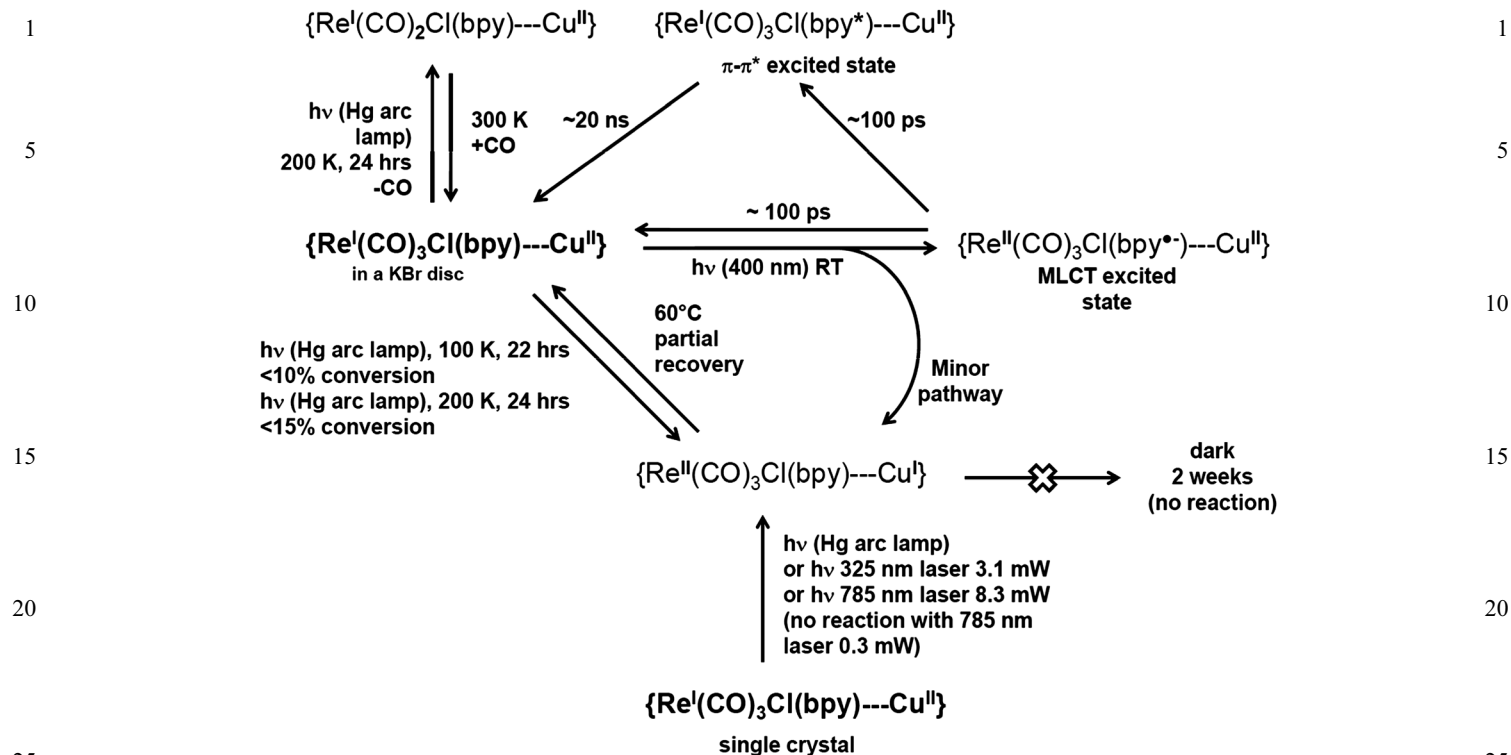


Fig. 1 Views of the single crystal structure of **ReCu** (a) fac-octahedral Re coordination sphere; (b) the five-coordinate Cu coordination sphere; (c) view along the crystallographic a -axis; (d) view along the crystallographic c -axis. In all figures guest DMF molecules are omitted for clarity. In parts (c) and (d) hydrogen atoms are omitted for clarity. Re – pink; Cu – orange; Cl – green; O – red; C – grey; N – blue; H – white.

formation of a $^3\text{MLCT}$ excited state. These transient bands are not stable and decay rapidly concurrently with partial reformation of the parent bands and with formation as a new species with bands shifted to lower energy (2008 and $\sim 1873 \text{ cm}^{-1}$) relative to the parent bands. These downshifted bands are consistent with formation of an intraligand (IL) $^3\pi-\pi^*$ excited state. The ps-kinetics of these species are shown in Fig. 2b: the growth of the IL $^3\pi-\pi^*$ state occurs with a lifetime of $102 \pm 15 \text{ ps}$ and the recovery of the ground state occurs with a lifetime of $105 \pm 10 \text{ ps}$, the bands due to the $^3\text{MLCT}$ state decaying biexponentially with these lifetimes. The TRIR obtained 6 ns after laser excitation shows only the IL $^3\pi-\pi^*$ excited state, which decays concurrently with reformation of the parent with a lifetime of 19 ns (Fig. 2c). These results are similar to those found when studying the **ReMn** MOF under the same conditions, the results suggesting that the IL $^3\pi-\pi^*$ excited state is lower than the $^3\text{MLCT}$ excited state.

An important difference between the **ReMn** and **ReCu** networks was observed when undertaking the TRIR experiments for prolonged periods of time. Typically, the data are collected using at least four ‘cycles’, each cycle consisting of a full data collection, the cycles then subsequently being



Scheme 1 Summary of experiments probing the nature of the excited states within ReCu and interplay between different states.

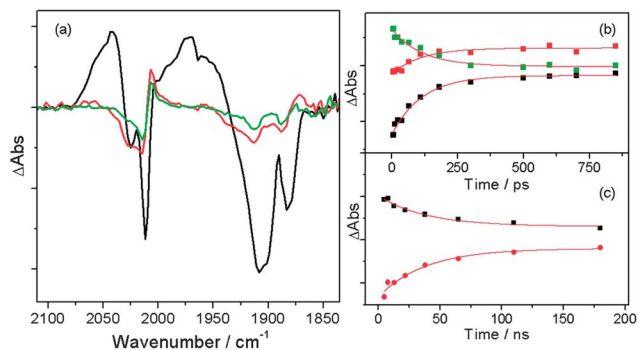


Fig. 2 (a) Difference IR spectra of ReCu in a KBr disc, recorded 3 ps (black), 500 ps (red) and 6 ns (green) after photolysis; (b) ps-kinetics recorded at 1909 cm^{-1} (black), 2007 cm^{-1} (red) and 2044 cm^{-1} (green); (c) ns-kinetics recorded at 2007 cm^{-1} (black) and 2015 cm^{-1} (red). Solid red lines correspond to exponential fits.

averaged. The **ReMn** network in KBr was completely photostable. The later cycles of the **ReCu** network in KBr, however, showed some small but important differences to the earlier cycles, in that new *bleach* bands began to appear, primarily at 2100 cm^{-1} and slightly shifted to higher energy than the parent $\nu(\text{CO})$ bands (Fig. 3a), perhaps consistent with the gradual and irreversible formation of a low quantum yield photoproduct with an absorption band concomitant with the laser excitation wavelength.

To investigate the photoproducts of the TRIR experiments, one of the KBr discs was analysed by FTIR after having been irradiated by the TRIR lasers. Fig. 3 shows the FTIR spectra of

the disc before and after the laser experiment. Clearly, new bands are observed in the $\nu(\text{CO})$ region at higher energy than the ground-state (2095, 2022 and 1940 cm^{-1} , Fig. 3b). An FTIR map of the disc was recorded (Fig. 3c) and plotted to show the integrated band intensity around the band at 2095 cm^{-1} . The red regions show areas of relatively high intensity and correspond to the three regions of 1 mm \times 1 mm irradiation over which the TRIR laser was rastered.

ReCu was photolysed in a KBr disc for 22 hours at 100 K and the UV/vis absorption (diffuse reflectance) and FTIR spectra were recorded at room temperature before and after photolysis (Fig. S1†). The UV/vis ground-state spectrum displays two broad, featureless absorbances centred around 440 and 685 nm. On photolysis, the 685 nm band is reduced in intensity and a new band appears, shown by the difference spectrum to be centred at 528 nm. This latter band is also responsible for the marked colour change of the sample from green to orange/brown in the irradiated region of the KBr disc. The FTIR spectra also display changes (Fig. S1c and d†), notably a reduction in the parent $\nu(\text{CO})$ band intensity and growth of weak bands shifted to higher energy at 2095 and 1948 cm^{-1} . These new bands are consistent with those observed at room temperature during the time-resolved experiments after the sample had been photolysed for a significant time and, coupled with the long photolysis time required at 100 K, again suggest a low quantum yield photoproduct. The shift in $\nu(\text{CO})$ to higher energy on formation of this new species is indicative of a greater reduction in electron density on the Re centre than seen on formation of the MLCT excited state and may be consistent with

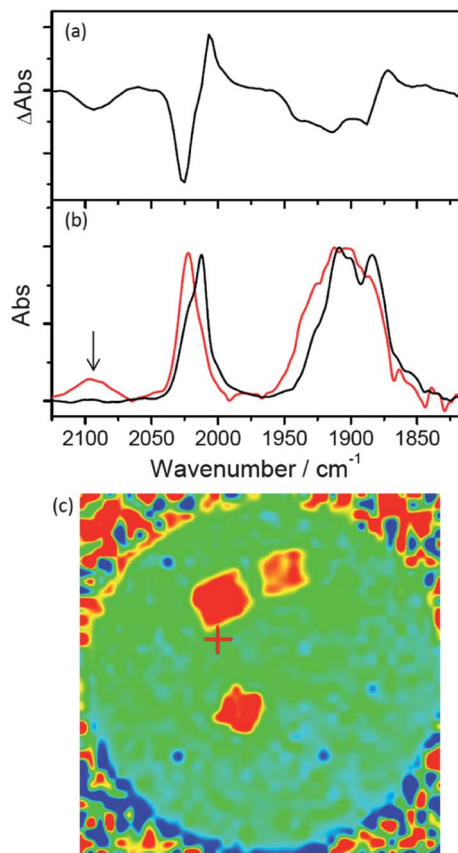


Fig. 3 (a) Difference IR spectrum of **ReCu** in a KBr disc which had been irradiated for a prolonged period in the TRIR experiments (see text), recorded 2 ns after excitation; (b) FTIR spectra before (black) and after (red) TRIR experiments, note new band at 2095 cm^{-1} ; and (c) FTIR-map of the disc after the TRIR experiments (see text).

the formal oxidation of the Re^{I} centre to Re^{II} . The changes seen may be indicative of a process whereby the excited state generated on the Re–diimine moiety partially decays by electron transfer to the Cu^{II} centre. The photoproduct of the 100 K KBr disc photolysis experiment was kept in the dark and the UV/vis and FTIR absorption spectra were recorded over the subsequent two weeks. No further significant spectral changes were observed in this time.

The UV/vis lamp photolysis of **ReCu** in a KBr disc was repeated at 200 K in an attempt to produce a higher yield of the photoproduct characterised by an FTIR absorbance around 2095 cm^{-1} . Fig. 4a shows the FTIR spectra obtained after 24 hours of photolysis of the disc at 200 K. The desired species with upshifted bands at 2095 , 2030 and 1936 cm^{-1} is formed in reasonable yield, and an additional pair of bands to lower energy than the parent $\nu(\text{CO})$ bands appears (at 1810 and *ca.* 1920 cm^{-1}). This latter pair of bands corresponds well to the spectra observed on low-temperature photolysis of the related **ReMn** species in KBr and can reasonably be assigned to the formation of a dicarbonyl species due to photodissociation of CO. This assignment is supported by the spectrum of **ReCu** in KBr recorded after warming the sample back to room temperature, in which the dicarbonyl $\nu(\text{CO})$ bands have decayed with a

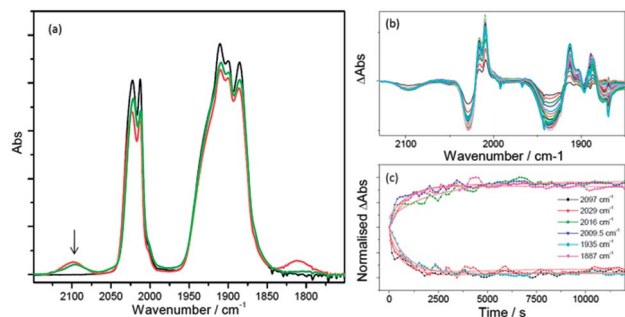


Fig. 4 (a) FTIR spectra of **ReCu** in a KBr disc at 200 K before photolysis (black), after 24 hours UV/vis photolysis (red) and after subsequent warming to 300 K (green), note new band at 2095 cm^{-1} ; (b) difference spectra on heating the photolysed disc to $60\text{ }^{\circ}\text{C}$, and (c) normalised kinetic traces recorded at the points shown at $60\text{ }^{\circ}\text{C}$ (red lines correspond to exponential fits).

simultaneous partial recovery of the parent bands. The upshifted $\nu(\text{CO})$ bands corresponding to the unidentified photoproduct are unsurprisingly still apparent.

Heating of the sample to $60\text{ }^{\circ}\text{C}$ and recording the temporal evolution of the spectra (Fig. 4b) reveals a partial loss of the photoproduct and return of the parent bands, but after approximately 90 min no further recovery was observed. This may indicate either a stable photoproduct or some decomposition process is occurring along with the partial recovery of the ground-state species. The tentative assignment of this photoproduct to an oxidised Re^{II} species based on the shift in $\nu(\text{CO})$ frequency is supported by the observation that electrochemical oxidation of $\text{Re}(\text{diimine})(\text{CO})_3\text{Cl}$ in solution is often irreversible, which may explain the lack of a complete recovery of the **ReCu** parent species in the FTIR experiments.

The oxidation of the Re^{I} centre to Re^{II} would be expected to be accompanied by reduction of the Cu^{II} centre on photolysis. Therefore pure **ReCu** crystals were examined by EPR spectroscopy. **ReCu** crystals are paramagnetic in the ground state, due to the presence of the $d^9\text{ Cu}^{\text{II}}$ centre, although $^{63/65}\text{Cu}$ ($I = 3/2$, 100%) hyperfine was not resolved (Fig. 5). On photolysis of a sample of **ReCu**, in a rotating EPR tube using a 125 W mercury

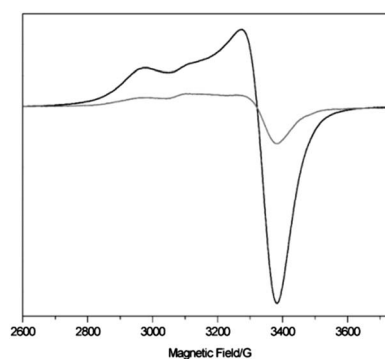


Fig. 5 EPR spectra before and after photolysis of the crystalline **ReCu** sample. The black spectrum corresponds to the ground-state/before photolysis EPR, and the grey line corresponds to the post-photolysis EPR spectrum.

lamp over a 9 hours period, the EPR signal is significantly reduced, reaching 25% of the original double integrated intensity, a result entirely in line with the conversion of Cu^{II} to diamagnetic Cu^{I} as postulated above. A simultaneous colour change is seen from green to orange/red, as also observed on irradiation of the complex in KBr discs. A series of EPR experiments were performed at ambient temperature on samples that had been maintained at temperatures from 20 °C to 80 °C (without photolysis) to determine the thermal stability of the ground-state **ReCu**, with no signal loss being observed purely on heating for extended periods of time (*ca.* 20 hours per sample) at temperatures up to and including 60 °C.

The essentially irreversible chemical modification of the network upon photoexcitation indicates that it may be possible to modify the nature of the crystal through the use of light, thereby facilitating writing on the crystal networks. We have used Raman spectroscopy to investigate changes in the $\text{Re}(\text{diimine})(\text{CO})_3\text{Cl}$ structure on photolysing **ReCu** single crystals. Interestingly, the use of 785 nm laser light as the Raman probe at high enough power was observed to convert the green crystals into badly cracked orange-brown crystals. Fig. 6 shows a single crystal before laser irradiation. Focusing the 785 nm laser ($\sim 3 \mu\text{m}$, 8.3 mW) on the crystal to obtain a Raman spectrum resulted in the production of darkened damaged spots (fine, localised fracturing of the crystal), and rastering the light in a line resulted in a darkened damaged line, Fig. 6b. In an attempt to reduce the damage further we rastered the laser in a $50 \times 50 \mu\text{m}$ square. However, this simply resulted in a darkened and cracked square, Fig. 6c, and the conversion process under these conditions was consistently found to damage the crystals to the point that crystallographic structure analysis of the photoproduct was not possible. FTIR analysis after photolysis showed that the photoproduct obtained following irradiation at 785 nm was the same as that produced by irradiating **ReCu** in KBr with a 125 W mercury lamp. A key feature of **ReCu**, however, is that the photolysis effect could be switched off completely by reducing the power level of the laser to 0.3 mW, allowing Raman spectra of the green ground-state **ReCu** to be collected, and strongly suggesting that the photo-conversion on irradiation at 785 nm is due to a 2-photon effect. Similarly, this effect was observed when irradiating the sample with the 660 nm and 532 nm lasers on the Raman spectrometer; higher power leads to crystal cracking.

The crystals were therefore irradiated using a 325 nm laser instead to initiate the photoprocess; optimising the conditions for laser photolysis lead to the conclusion that the 325 nm laser (3.1 mW) could be used to optically 'write' on the **ReCu** crystals

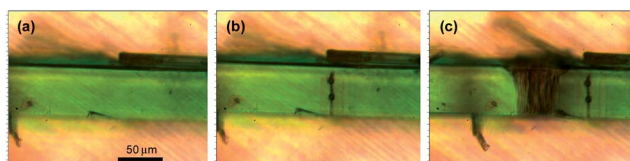


Fig. 6 Optical images of a crystal of **ReCu** (a) before irradiation with 785 nm laser light from the Raman spectrometer; (b) after irradiation in two spots and along a vertical line (2 seconds, 8.3 mW), and (c) after irradiation rastered over a $50 \times 50 \mu\text{m}$ square (20 seconds).

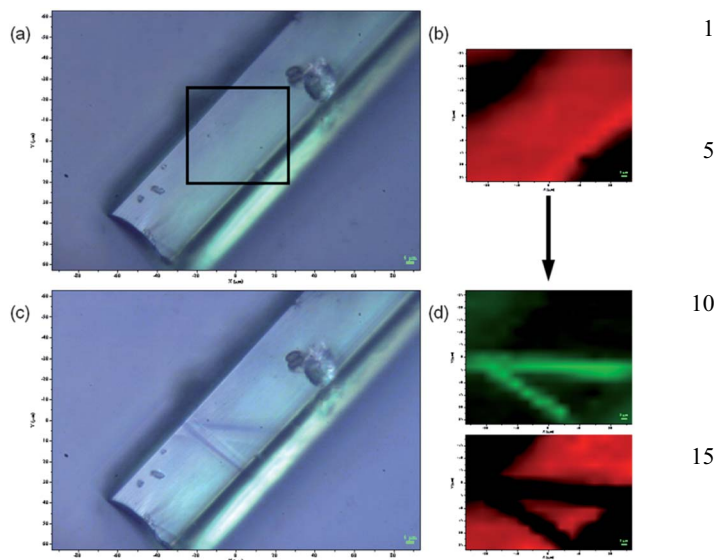


Fig. 7 Single crystal photolysis and mapping of **ReCu** showing (a) the crystal before irradiation, the black box representing (b) the area mapped by Raman spectroscopy, red corresponding to the presence of the ground state Raman spectrum; (c) The crystal after two lines have been 'written' and (d) the Raman spectral intensity and spatial distribution of the ground-state Raman spectrum (red) and the photoproduct Raman spectrum (green).

and the 785 nm laser (at low power) could be used to map any changes in the Raman spectrum (Fig. S2†). Since the crystals are typically 40–50 μm in their smallest dimension and the laser spot size is in the order of one micron, it was decided to use the piezo-controlled mirrors on the Raman spectrometer to sweep the beam back and forth across the crystal at relatively low power over a 2 hours period, to minimise significant damage to integrity of the crystal, mapping the area before and after photolysis. Two sweeps of 2 hours each at 45° to each other† were attempted and the results are shown in Fig. 6. The darkening of the crystal along the lines of photolysis is clearly visible (Fig. 7b) and the before and after Raman spectroscopy maps show the distribution of photoproduct to be entirely along the line of photolysis. The ability to evaluate the position of photolysis by Raman spectroscopy demonstrates that our approach not only allows us to write on the crystal but also to read that information from the crystal.

Conclusions

Our study demonstrates the potential utility of carefully designed coordination networks in the development of novel photoactive materials. The building-block approach¹⁸ to preparing coordination networks, or MOFs, allows organisation of the relative placement of chemical components in the network structure, facilitating arrangement of photo- or redox-active species in defined arrays. This study demonstrates the interplay between such components which we have exploited to develop a method of writing on crystal surfaces. We believe our study opens up a new direction for network materials which we are currently developing and expanding.

Acknowledgements

The authors gratefully acknowledge the support of the Engineering and Physical Sciences Research Council (EP/D058147/1) for funding and STFC for the award of beamtime on SRS Station 9.8. NRC and MWG gratefully acknowledge receipt of a Royal Society Wolfson Merit Awards.

Notes and references

‡ Two distinct directions of photolysis were used to rule out any possible dependence on crystal orientation.

1 N. R. Champness, *Dalton Trans.*, 2011, **40**, 10311–10315.

2 The terminology of coordination polymers/networks and MOFs is a matter of some debate; we have used the term coordination network to describe the materials described herein, directing the reader toward the specific properties of this system and avoiding confusion with properties commonly associated with MOFs. For further discussion on this topic the reader is referred to the following article: S. R. Batten, N. R. Champness, X.-M. Chen, J. Garcia-Martinez, S. Kitagawa, L. Ohrstrom, M. O'Keeffe, M. P. Suh and J. Reedijk, *CrystEngComm*, 2012, **14**, 3001–3004; S. R. Batten, N. R. Champness, X.-M. Chen, J. Garcia-Martinez, S. Kitagawa, L. Öhrström, M. O'Keeffe, M. P. Suh and J. Reedijk, *Pure Appl. Chem.*, 2013, **85**, 1715–1724.

3 M. Kurmoo, *Chem. Soc. Rev.*, 2009, **38**, 1353–1379.

4 X. Lin, N. R. Champness and M. Schröder, *Top. Curr. Chem.*, 2010, **293**, 35–76.

5 A. J. Blake, N. R. Champness, T. L. Easun, D. R. Allan, H. Nowell, M. W. George, J. Jia and X.-Z. Sun, *Nat. Chem.*, 2010, **2**, 688–694.

6 H. Sato, R. Matsuda, K. Sugimoto, M. Takata and S. Kitagawa, *Nat. Mater.*, 2010, **9**, 661–666.

7 K. K. Tanabe, C. A. Allen and S. M. Cohen, *Angew. Chem., Int. Ed.*, 2010, **49**, 9730–9733.

8 S. S. Kaye and J. R. Long, *J. Am. Chem. Soc.*, 2008, **130**, 806–807.

9 C. Y. Lee, O. K. Farha, B. J. Hong, A. A. Sarjeant, S. T. Nguyen and J. T. Hupp, *J. Am. Chem. Soc.*, 2011, **133**, 15858–15861.

10 A. Fateeva, P. A. Chater, C. P. Ireland, A. A. Tahir, Y. Z. Khimiyak, P. V. Wiper, J. R. Darwent and M. J. Rosseinsky, *Angew. Chem., Int. Ed.*, 2012, **51**, 7440–7444.

11 (a) C. A. Kent, B. P. Mehl, L. Ma, J. M. Papanikolas, T. J. Meyer and W. Lin, *J. Am. Chem. Soc.*, 2010, **132**, 12767–12769; (b) C. A. Kent, D. Liu, L. Ma, J. M. Papanikolas, T. J. Meyer and W. Lin, *J. Am. Chem. Soc.*, 2011, **133**, 12940–12943; (c) C. Wang, Z. G. Xie, K. E. deKrafft and W. Lin, *J. Am. Chem. Soc.*, 2011, **133**, 13445–13454.

12 Y. Takashima, V. M. Martínez, S. Furukawa, M. Kondo, S. Shimomura, H. Uehara, M. Nakahama, K. Sugimoto and S. Kitagawa, *Nat. Commun.*, 2011, **2**, 168.

13 C. Wang and W. Lin, *J. Am. Chem. Soc.*, 2011, **133**, 4232–4235.

14 M. D. Ward, *Nat. Chem.*, 2010, **2**, 610.

15 (a) S. K. Brayshaw, T. L. Easun, M. W. George, A. M. E. Griffin, A. L. Johnson, P. R. Raithby, T. L. Savarese, S. Schiffers, J. E. Warren, M. R. Warren and S. J. Teat, *Dalton Trans.*, 2012, **41**, 90–97; (b) M. R. Warren, S. K. Brayshaw, A. L. Johnson, S. Schiffers, P. R. Raithby, T. L. Easun, M. W. George, J. E. Warren and S. J. Teat, *Angew. Chem., Int. Ed.*, 2009, **48**, 5711–5714.

16 (a) S. Kobatake, S. Takami, H. Muto, T. Ishikawa and M. Irie, *Nature*, 2007, **446**, 778–781; (b) L. Zhu, R. O. Al-Kaysi and C. J. Bardeen, *J. Am. Chem. Soc.*, 2011, **133**, 12569–12575.

17 (a) H. Wu, J. Yang, Z.-M. Su, S. R. Batten and J.-F. Ma, *J. Am. Chem. Soc.*, 2011, **133**, 11406–11409; (b) S. T. Hyde, M. O'Keeffe and D. M. Proserpio, *Angew. Chem., Int. Ed.*, 2008, **47**, 7996–8000.

18 B. F. Hoskins and R. Robson, *J. Am. Chem. Soc.*, 1990, **112**, 1546–1554.